

Non-existence of the s-f transition in structures of solid gadolinium at pressure

Qingchen Li, Hossein Ehteshami, Keith Munro, Malcolm I McMahon and Graeme J. Ackland*

¹Centre for Science at Extreme Conditions and School of Physics and Astronomy,
University of Edinburgh, Edinburgh, U.K. EH9 3FD

(Dated: November 18, 2021)

Gadolinium has long been believed to undergo a high pressure volume collapse transition like cerium, with an electron transferring from the extended *s*-orbital to the compact *f*-orbital. However, experimental measurement has been unable to detect any associated change in the magnetic properties of the *f*-electrons¹. Here we resolve this discrepancy by showing that there is no significant volume collapse. We present density functional theory calculations of solid gadolinium under high pressure using a range of methods, and revisit the experimental situation using X-ray diffraction. The standard lanthanide pressure-transformation sequence involving different stackings of close-packed planes: *hcp* → *9R* → *dhcp* → *fcc* → *d-fcc* is reproduced. The so-called “volume collapsed” high-pressure phase, is shown to be an unusual stacking of close-packed planes, with *Fddd* symmetry and a density change less than 1%. The distorted fcc (d-fcc) structure is revealed to arise as a consequence of antiferromagnetism. The results are shown to be remarkably robust to various treatments of the *f*-electrons, which we therefore conclude do not participate in the bonding.

Over the last 30 years, calculations of high pressure phases using density functional theory (DFT) and the Kohn-Sham Hamiltonian have shown a remarkable level of agreement with experiment. This occurs despite the very simple quasi-local approximations used for the exchange-correlation interactions, such as the local density (LDA) and generalized gradient approximations (GGA). Crystal structure prediction^{2,3} is a particularly forgiving problem for DFT, because there is no explicit dependence of the exchange correlation energy on the atomic positions⁴⁻⁷.

A notable exception to the rule has been so-called “strongly correlated” systems, typically those where integer numbers of electrons are localised on particular atoms. For example, iron oxides are wrongly predicted to be metallic with LDA/GGA, a situation which required fixes such as adding some arbitrary amount of Hartree-Fock exchange⁸, or a Hubbard *U* term to force the *d*-electrons to remain localised below the Fermi energy^{9,10}. It has generally been assumed that the problems encountered with *d*-electrons would be even more severe in materials with *f*-electrons, such as lanthanides.

The lanthanides (Ce to Lu) are characterised by the increasing number of *4f* electrons which, following Hund’s rules, adopt the highest possible value of spin. The high stability of the filled spin-up *f*-shell means that both Eu and Gd have 7 *f*-electrons with spin 7/2. At ambient pressure, the *f*-electron states lie far from the Fermi level and the bonding is dominated by the *s* and *d* bands: this gives rise to a common pressure-induced phase transition sequence comprising different stackings of close-packed layers: *hcp* (space group *P63/mmc*, hP2 in Pearson notation, and *h* in close-packed stacking notation¹¹) → *9R* (*R3m*, hR3, *hhf*) → double-*hcp* (*P63/mmc* hP4, *hf*) → *fcc* (*Fm3m* cF4, *f*). The close-packed stacking notation reveals a monotonic tendency away from *hcp*-like *ABA* stackings toward *ABC*-type stacking with pressure, a trend which is also observed with reducing atomic number, to the extent that *hcp* does not occur in Sm ex-

cept at high temperature, and *9R* is also absent from Ce to Pm. At elevated temperatures, the bcc structure may be observed. At still higher pressure a distorted-fcc (*R3m* and *hR24*) structures appears. There are no significant volume changes between any of these different close packed phases. In previous experiments on Gd¹²⁻¹⁵, not all transformations were identified, e.g. missing *hcp*¹³, missing *fcc*¹⁴, and in the most recent study¹⁵ *9R* is not observed.

The similarity between all these elements suggests that the *f*-electrons do not play a central role in determining crystal stability. However, at much higher pressures all the lanthanides were believed to undergo a “volume-collapse” transition to a denser but non-close packed structure. An obvious cause for such a transition would be the transfer of electrons from delocalised states into the tightly-bound *f*-state¹⁶⁻²⁰ - exactly the type of process which DFT describes badly¹⁴.

The three most popular theoretical explanations for such a pressure-induced collapse are

- the *s-f* valence transition model²¹, in which a conduction band electron is transferred into the *f*-band causing a reduction in the ionic radius;
- the Mott-Hubbard model²² where the *4f* states undergo a local-to-itinerant transition, leading to a significant contribution to crystalline binding
- the Kondo volume collapse model²³, where the localized *4f* level approaches the Fermi energy giving a sharp increase in the Kondo temperature.

The *4f* electrons play a critical role in all cases. However, experimental X-ray absorption and emission spectroscopy¹ showed that the *f*-electrons were largely unaffected by the transformation.

Our recent high pressure X-ray data led to a revised picture for the collapsed phases across the lanthanides²⁴. An entirely new family of crystal structures was revealed: based on quasi-close packed layers where each successive

layer has atoms situated above the mid-point between two atoms in the preceding layer, resulting in 10-fold coordination. By analogy with the ABC notation for close packing the observed structures were labelled ABCAD-CBD (Tb) ABCD (Pu) ABC (Sm), and the possibility of other, short-repeat, stackings noted. These structures were shown to be a better fit to the X-ray data than the previously-assumed body-centred monoclinic, C2/m or mC4 structures^{14,15,25}. In addition to having no layer repeats (e.g. AA is forbidden), we note that these stacking structures all satisfy an additional condition that each layer is different from either of the TWO below it, (ABA is forbidden). This allows a concise notation to uniquely categorize the structures, labelling each layer by

- 0 = same as three layers below
- 1 = different from three layers below

In this notation, the three observed structures are the simplest ($ABCADCBD \rightarrow 10$, $ABCD \rightarrow 1$, $ABC \rightarrow 0$), whereas shorter sequences become longer (eg $ABCDB \rightarrow 11110$).

Using a combination of the hf notation for close packing, which explains the sequence¹¹, and this 01 notation for the new family, we can comprehensively study the possible structures adopted by Gd. A previous study included electronic structure calculations using Dynamical Mean-Field Theory (DFT+DMFT) to focus on the band structure and the f -electrons. The DMFT enables a detailed treatment of the unscreened moments, which were believed to be “*key for the correct description of the structure at high pressure.*”²⁴. This belief arose because the volume collapse mechanism of $s - f$ transfer obviously requires a correct treatment of the f -electrons. However, the DMFT method was found to have instabilities as shown by the thermodynamically-impossible discontinuity of Gibbs free energy in the DMFT-calculated enthalpy-pressure relation²⁴.

We approach the problem from the opposite end. Rather than using the most sophisticated treatment available, we ask how simple can a DFT calculation be, while still obtaining the correct series of phases transformations. This approach will demonstrate which aspects of the physics are essential to understanding the sequence. We choose to examine gadolinium, because its half-filled f -shell is likely to be most amenable to a simple treatment.

We used the CASTEP code with ultrasoft pseudopotentials and PBE^{7,26-28} functional. We treated the $5s5p4f6s5d$ and above electrons as valence, giving 18 explicitly calculated electron states per atom. We used a plane wave basis set with a 425eV cutoff. We also considered use of a Hubbard- U which will have the effect to localize, but not split, the f -electrons. The Hubbard- U is generally regarded as the minimal plausible theory for f -electrons, with a typical value of $U = 6.7\text{eV}$ ²⁹ giving a good fit to the experimentally determined electronic structure.

The simplest level of theory, non-magnetic calculations, results in an f -band at the Fermi surface. This is clearly incorrect, so all calculations presented here allow for spin dependence²⁶.

At ambient pressure Gd has a ferromagnetic hcp structure with a Curie temperature of 293K³⁰, with some susceptibility anomalies^{31,32}. On further increase in pressure the situation is unclear, but may be similar to Sm which exhibits layered antiferromagnetic structures at pressure with a Neel temperature around 60K³³. Consequently, in our calculations we consider both ferromagnetic and various antiferromagnetic versions of each structure (Details in supplemental materials).

Figure.1 shows that using this value of U gives the typical sequence of phase transformations, with the exception that 9R is slightly too high in energy. An example of the density of states is shown in Figure 3. The f -electrons are split into a spin-up and spin-down band, well above and below the Fermi energy. By projecting the wavefunctions onto localised orbitals, we find that the valence states have hybrid $s - d$ character. There is no splitting within the f -electrons levels of the same-spin, in contrast to the DMFT result²⁴. We can therefore conclude that *the sequence of crystal structures does not depend on the accurate treatment of f -electrons.* Most remarkably, the observation also applies to the volume-collapsed phase.

It is interesting to note the similar shape of the majority and minority spin bands in hcp, aside from a shift which places the Fermi level in a density of states minimum. It suggests the that, in addition to the localised f -magnetisation, the hcp structure exhibits Stoner-type sd -ferromagnetism³⁴.

To investigate further, we varied the value of U , giving a progressively poorer treatment of the f -electrons. Even more remarkably, this *still* does not affect the sequence of phase transformations, even when the U is absent altogether (see Supplemental Materials).

The calculations allow us to make some observations about the nature of the structures. At 0GPa, all the close packed structures were found to be ferromagnetic within their range of stability, except for fcc. Above 45GPa ferromagnetic fcc becomes unstable with respect to antiferromagnetic ordering. However, it is impossible to decorate the fcc lattice with spins while maintaining the cubic symmetry, and on relaxing the atomic positions in the antiferromagnetic supercell they move away from fcc. This provides an elegant explanation for the transition to the distorted-fcc phase: it is the structural signature of a magnetic phase transition. Such magnetic symmetry breaking in metals can be described by antiferromagnetic Ising model³⁵ which implies that there is a paramagnetic phase at elevated temperature, a likely candidate for the Gd IX phase.

We estimated the paramagnetic transitions using the effective mean field (EMF) approach assuming Ising spins^{36,37} with coupling constant J . DFT calculations on hcp at zero pressure showed that, compared to FM phase

which has a ground state Ising enthalpy $H_{Is} = -6J$, the AFM structures are higher in energy by 36meV/atom (layered, P-6m2 symmetry, $U=0$) 38meV/atom (striped, Pmmn symmetry, $H_{Is}=0$) and 53meV/atom (striped, Pmma symmetry, $H_{Is}=2J$). This implies a value for $J \sim 6\text{meV}$ with an associated Curie temperature $T_c = 11J \sim 800\text{K}$. This estimated value of T_c is very sensitive to assumptions: an identical calculation at the experimental density gives a value some 20% lower, fitting a second neighbour model gives a similar reduction and the experimental value is 293K³⁸⁻⁴⁰. The lowest energy structure we found among the many possible AFM 9R structures is ferrimagnetic, with the (two) h and (one) f layers having opposite spin. All the structures considered lie within 10meV per atom, implying a Neel temperature $T_N = 1.7J \sim 50\text{K}$. dhcp is also antiferromagnetic, with a similarly low Neel temperature. We also note that the AFM configurations are typically 0.5% denser than the ferromagnetic ones, due to fewer exchange repulsions and resulting in the negative linear thermal expansion coefficient in the c -direction.

Figure 4 shows the effect of adding the EMF^{36,37} free energy to the zero-K DFT data. The EMF is precise, but the uncertainty in the parameters implies errors in the transition temperature of hundreds of Kelvin.

A further small correction to the free energy difference comes from phonon free energy. We calculated this using finite displacement method^{41,42} in CASTEP²⁷, and found a contribution to free energy difference around 2 meV/atom at room temperature, which could shift the phase transition pressure by a few GPa. (see Supplemental materials). Again, 9R is favored over hcp.

The ‘‘collapsed’’ $Fddd$ phase becomes stable over d-fcc above 85GPa. However, in our calculation the difference in density between d-fcc and $Fddd$ is less than 1%: the calculations *do not predict a volume collapse*. Moreover, the electronic density of states for $Fddd$ shows that the f -electrons lie well below the Fermi surface.

Previous evidence for ‘‘volume collapse’’ transitions in the lanthanides has been based on X-ray diffraction (XRD) measurements. However, XRD is not a direct measure of density: it is necessary to know the crystal structure, and we have also reexamined the experimental situation. Room temperature angle-dispersive x-ray diffraction experiments were performed on the high-pressure beamline I15 at the Diamond Light Source using diamond anvil cells and a MAR345 detector. Samples were cut from 99.99% purity Gd ingots, two contaminants phases were identified in the diffraction patterns, each of which could be fitted with the fcc structure and then eliminated from the Rietveld refinement of diffraction profiles from the pure Gd. The full experimental details are published elsewhere⁴³.

The as-loaded sample showed a number of peaks which could not be accounted for by the hcp phase, and there

were assigned to the 9R phase. The 9R-dhcp transformation was first detected at 8.9 GPa and found to be complete by 10.2 GPa. The dhcp phase transformed directly into the d-fcc phase at 33.6 GPa, by-passing the fcc phase completely, similar to the results reported by Hua et al.¹⁴ We found that the previously-assumed monoclinic $mC4$ structure is incorrect. The ‘‘volume collapsed’’ phase, is now identified as $Fddd$, which enabled us to reexamine the equation of state. Fig.2 shows a waterfall plot of diffraction data across the d-fcc \rightarrow $Fddd$ transformation, and compares the implied experimental equation of state with the DFT calculation. DFT calculations show the $mC4$ structure to be very high in energy. The key result is that *there is no experimental evidence for volume collapse in Gadolinium*.

In sum, we have presented a series of DFT calculations of high pressure phases in gadolinium. These have shown that, despite the difficulty of describing localised f -states in DFT, the correct sequence of structures can be obtained using this method. This indicates that the f -electrons do not play a role in the phase stability.

Treating the phases as antiferromagnetic is important, and both sd and f bands exhibit magnetization. The distorted-fcc phase is shown to be a consequence of the frustration of antiferromagnetism of that lattice. All high-pressure phases apart for hcp are predicted to be antiferromagnetic. DFT+ U calculation even applies to the ‘‘volume-collapsed’’, phases which were previously associated with $s - f$ electron transfer. Furthermore, they predict that there is no significant, volume collapse - a finding borne out by the recent revision of the high-pressure crystal structure. This work explains the failure of magnetic susceptibility experiments to verify any of the rival theories of $s - f$ electron transfer at volume collapse: neither exist.

We have concentrated here on gadolinium, because the half-filled f -band facilitates the simple DFT treatment, but we expect the same physical principles to apply to the other lanthanides.

$hcp \rightarrow$	9R	dhcp	fcc	d-fcc	Fddd
h	hhf	hf	f	f	01
Errandonea	2	6	26	33	60.5
Samudrala	2	6.5	25	31	61
Expt	0	10	-	33.6	73
Calc (FM)	-	11	33	-	90
Calc (AFM)	-	10	30	40	113

TABLE I: 0K DFT transition pressures in GPa. The calculated $hcp \rightarrow 9R$ transformation pressure is above $hcp \rightarrow dhcp$, so 9R has no predicted region of stability at 0K.

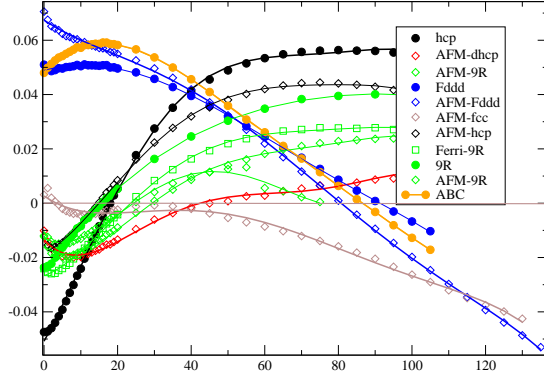


FIG. 1: 0-K calculated enthalpy for various phases relative to ferromagnetic fcc. Filled circles show ferromagnetic phases, open ones AFM. The implied sequence of phase transitions is hcp (black) -dhcp (red) - fcc (brown) -Fddd (blue). The 9R phase (green, see Supplemental materials for AFM definitions) has a slope intermediate between hcp and dhcp, but is only metastable in these calculations. Antiferromagnetism breaks fcc symmetry, so AFM-fcc has a small distortion from fcc, referred to as d-fcc. At higher temperatures the paramagnetic 9R and fcc also have regions of stability.

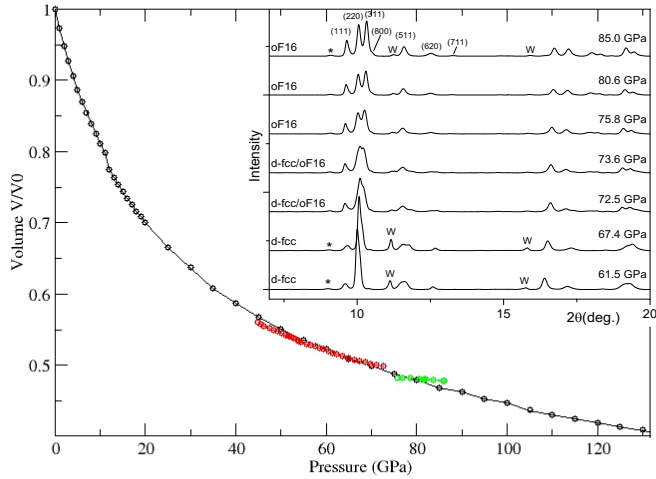


FIG. 2: Equation of state for the various phases hcp-dhcp-fcc-dfcc-Fddd comparing calculation with experiment $EoS^{15,43}$. The calculated V_0 is $35.67 \text{ \AA}^3/\text{atom}$, while the experimental value is $33.10 \text{ \AA}^3/\text{atom}$ - the difference corresponds to a 3 GPa pressure error in the calculation, similar to the offset of the hcp-9R transition. The inset shows a waterfall plot of integrated diffraction profiles obtained from Gd between 61 and 85 GPa, illustrating the d-fcc \rightarrow Fddd transition at ~ 73 GPa. The low-angle peaks in the Fddd phase at 85 GPa are indexed according to Pearson notation $oF-16$. Peaks from the tungsten gasket and from a minority contaminant phase are identified with 'W' and asterisks, respectively.

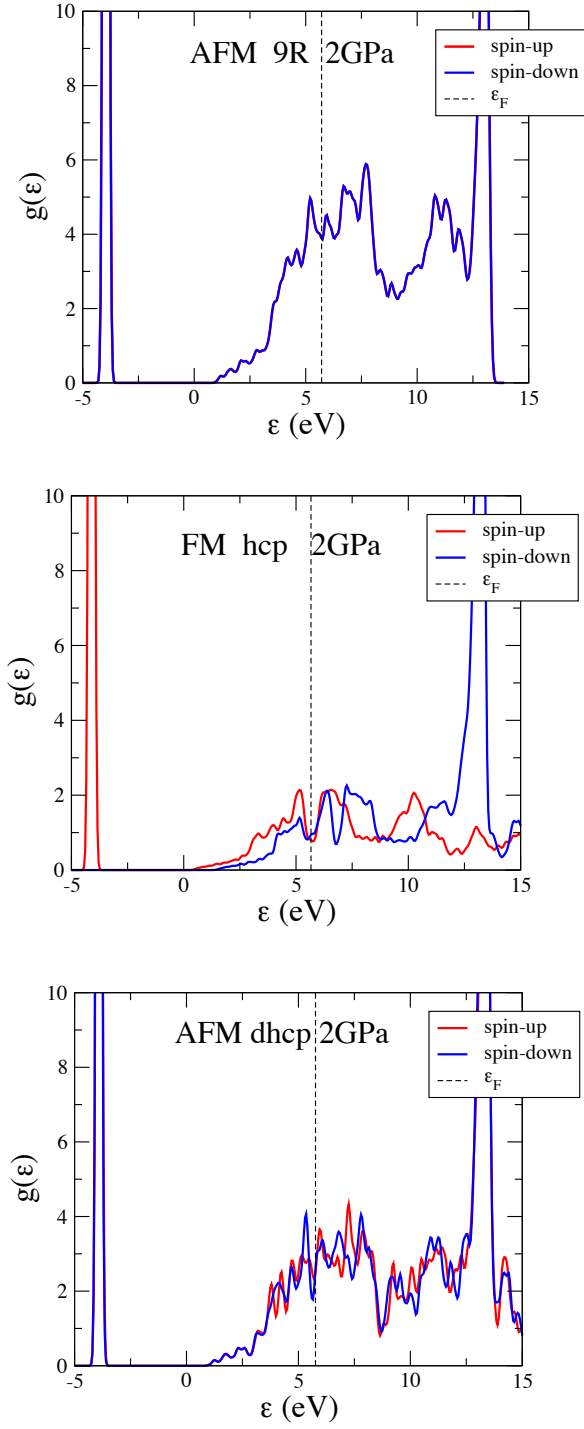


FIG. 3: Calculated Density of States per unit cell for three competing structures at 2GPa. (a) antiferromagnetic 9R (b) Ferromagnetic hcp (c) antiferromagnetic dhcp. The very sharp peak corresponding to the half-filled f -band lies well below E_F , with the unfilled f -band well above E_F . States around the Fermi level have hybrid $s-d$ character.

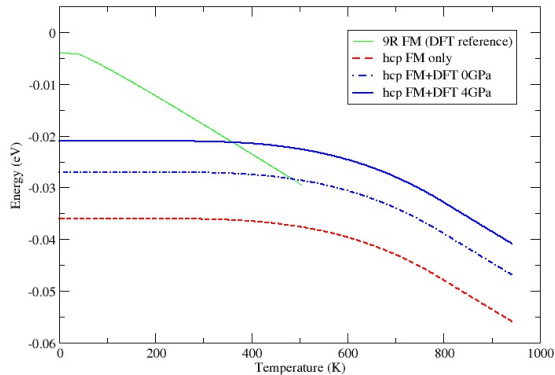


FIG. 4: Effect of magnetic free energy in stabilizing 9R phase. Magnetic free energy is calculated assuming values of $J = -6\text{meV}$ for hcp (red, dashed) and $+2\text{meV}$ for 9R (green, solid), blue lines show the effect of aligning the free energy difference at $T=0$ with the DFT data. 4GPa is chosen as the pressure which gives the experimental volume at the hcp-9R transition. Including the phonon free energy would raise the hcp curves by about 0.002eV , stabilizing and lowering the transformation temperature of 9R slightly.

* g.j.ackland@ed.ac.uk

- ¹ G. Fabbri, T. Matsuoka, J. Lim, J. R. L. Mardegan, K. Shimizu, D. Haskel, and J. S. Schilling, *Physical Review B* **88**, 245103 (2013).
- ² C. J. Pickard and R. J. Needs, *Journal of Physics: Condensed Matter* **23**, 053201 (2011).
- ³ Y. Wang, J. Lv, L. Zhu, and Y. Ma, *Computer Physics Communications* **183**, 2063 (2012).
- ⁴ P. Hohenberg and W. Kohn, *Physical review* **136**, B864 (1964).
- ⁵ W. Kohn and L. J. Sham, *Physical review* **140**, A1133 (1965).
- ⁶ J. P. Perdew and M. Levy, *Physical Review Letters* **51**, 1884 (1983).
- ⁷ J. P. Perdew, K. Burke, and M. Ernzerhof, *Physical review letters* **77**, 3865 (1996).
- ⁸ J. P. Perdew, M. Ernzerhof, and K. Burke, *The Journal of chemical physics* **105**, 9982 (1996).
- ⁹ J. Hubbard, *Proceedings of the Royal Society of London. Series A. Mathematical and Physical Sciences* **276**, 238 (1963).
- ¹⁰ Y. Meng, X.-W. Liu, C.-F. Huo, W.-P. Guo, D.-B. Cao, Q. Peng, A. Dearden, X. Gonze, Y. Yang, J. Wang, et al., *Journal of chemical theory and computation* **12**, 5132 (2016).
- ¹¹ C. H. Loach and G. J. Ackland, *Physical Review Letters* **119**, 205701 (2017).
- ¹² L. Xiong, J. Liu, L. Bai, X. Li, C. Lin, and J.-F. Lin, *Journal of Applied Physics* **116**, 243503 (2014).
- ¹³ J. Akella, G. S. Smith, and A. P. Jephcoat, *Journal of Physics and Chemistry of Solids* **49**, 573 (1988).
- ¹⁴ H. Hua, Y. K. Vohra, J. Akella, S. T. Weir, R. Ahuja, and B. Johansson, *The Review of High Pressure Science and Technology* **7**, 233 (1998).
- ¹⁵ D. Errandonea, R. Boehler, B. Schwager, and M. Mezouar, *Physical Review B* **75**, 014103 (2007).
- ¹⁶ B. Maddox, A. Lazicki, C. Yoo, V. Iota, M. Chen, A. McMahan, M. Hu, P. Chow, R. Scalettar, and W. Pickett, *Physical review letters* **96**, 215701 (2006).
- ¹⁷ C.-S. Yoo, B. Maddox, and V. Iota, *MRS Online Proceedings Library Archive* **1104** (2008).
- ¹⁸ G. K. Samudrala, G. M. Tsoi, S. T. Weir, and Y. K. Vohra, *High Pressure Research* **34**, 385 (2014).
- ¹⁹ J. Lim, G. Fabbri, D. Haskel, and J. Schilling, in *Journal of Physics: Conference Series* (IOP Publishing, 2014), vol. 500, p. 192009.
- ²⁰ N. K. Sarvestani, A. Yazdani, and S. Ketabi, *Physical Chemistry Chemical Physics* **16**, 25191 (2014).
- ²¹ R. Ramirez and L. M. Falicov, *Physical Review B* **3**, 2425 (1971).
- ²² B. Johansson, *Philosophical Magazine* **30**, 469 (1974).
- ²³ J. W. Allen and R. M. Martin, *Physical Review Letters* **49**, 1106 (1982).
- ²⁴ M. I. McMahon, S. Finnegan, R. J. Husband, K. A. Munro, E. Plekhanov, N. Bonini, C. Weber, M. Hanfland, U. Schwarz, and S. Macleod, *Physical Review B* **100**, 024107 (2019).
- ²⁵ R. J. Husband, I. Loa, G. W. Stinton, S. R. Evans, G. J. Ackland, and M. I. McMahon, *Physical Review Letters* **109**, 095503 (2012).
- ²⁶ M. D. Segall, P. J. D. Lindan, M. J. Probert, C. J. Pickard, P. J. Hasnip, S. J. Clark, and M. C. Payne, *Journal of*

- Physics: Condensed Matter **14**, 2717 (2002).
- ²⁷ S. J. Clark, M. D. Segall, C. J. Pickard, P. J. Hasnip, M. I. Probert, K. Refson, and M. C. Payne, *Zeitschrift für Kristallographie-Crystalline Materials* **220**, 567 (2005).
- ²⁸ D. Vanderbilt, *Physical Review B* **41**, 7892 (1990).
- ²⁹ L. Oroszlány, A. Deák, E. Simon, S. Khmelevskiy, and L. Szunyogh, *Physical Review Letters* **115**, 096402 (2015).
- ³⁰ D. R. Lide, *Handbook of Chemistry and Physics* **81** (2005).
- ³¹ S. N. Kaul and S. Srinath, *Physical Review B* **62**, 1114 (2000).
- ³² J. M. D. Coey, V. Skumryev, and K. Gallagher, *Nature* **401**, 35 (1999).
- ³³ Y. K. Vohra, G. M. Tsoi, and C. R. Johnson, *Journal of Physics: Condensed Matter* **29** (2016).
- ³⁴ E. C. Stoner and E. Wohlfarth, *Philosophical Transactions of the Royal Society of London. Series A, Mathematical and Physical Sciences* **240**, 599 (1948).
- ³⁵ G. J. Ackland, *Physical Review Letters* **97**, 015502 (2006).
- ³⁶ H. Ehteshami and G. J. Ackland, *Journal of Physics: Condensed Matter* **32** (2020).
- ³⁷ R. Honmura and T. Kaneyoshi, *Journal of Physics C: Solid State Physics* **12**, 3979 (1979).
- ³⁸ C. Graham Jr, *Journal of Applied Physics* **36**, 1135 (1965).
- ³⁹ V. V. Vorobev, Y. N. Smirnov, and V. A. Finkel, *Soviet Physics JETP* **22**, 1212 (1966).
- ⁴⁰ V. A. Finkel and V. S. Belovol, *Soviet Physics JETP* **34** (1972).
- ⁴¹ M. C. Warren and G. J. Ackland, *Physics and Chemistry of Minerals* **23**, 107 (1996).
- ⁴² G. J. Ackland, M. C. Warren, and S. J. Clark, *Journal of Physics: Condensed Matter* **9**, 7861 (1997).
- ⁴³ K. A. Munro, *Edinburgh Research Archive* **1842**, 28881 (2017), URL <https://era.ed.ac.uk/handle/1842/28881>.

Acknowledgments

GJA and HE acknowledge the support of the European Research Council Grant Hecate Reference No. 695527. GJA acknowledges a Royal Society Wolfson fellowship. EPSRC funded studentships for KM, computing time (UKCP grant P022561). MIM is grateful to AWE for the award of a William Penney Fellowship. The computational work was supported by the ARCHER UK National Supercomputing Service.

Supplemental Materials

S1. Effect of Hubbard U

We used PBE+U to "force" the f -electrons to localise. For the main calculations, we set $U=6.7\text{eV}$. In Fig.S5 we show the effect of changing U on the density of states, calculated for the AFM-Fddd phase at 90GPa. The very sharp peak corresponding to the half-filled f -band lies well below E_F , and the main effect of $+U$ is to shift this peak. The simple treatment means that the peak is not split, however the figures show that it does not broaden, hybridize or contribute to the valance band. Consequently, the value of U it has no significant effect on the energy differences between phases and the phase transformation sequence. The largest effect is at the Fddd-fcc transformation, where increase U from 0 to 8eV shifts the enthalpy difference by 10meV, in favour of fcc, and the predicted phase transformation pressure by about 10GPa. Interestingly, the f -band remains localised even with $U = 0$, so the use of the Hubbard U does not affect the conclusions of this paper. The occupied f -states lie below the sd -band, forming a sharp peak in the DoS. The unoccupied f -states are well above the Fermi energy, but lie within the sd -band, appearing as a distinct but broader peak. Regardless of the choice of U , the f -band does move closer to E_F with pressure, and this is essentially unaffected by the crystal structure.

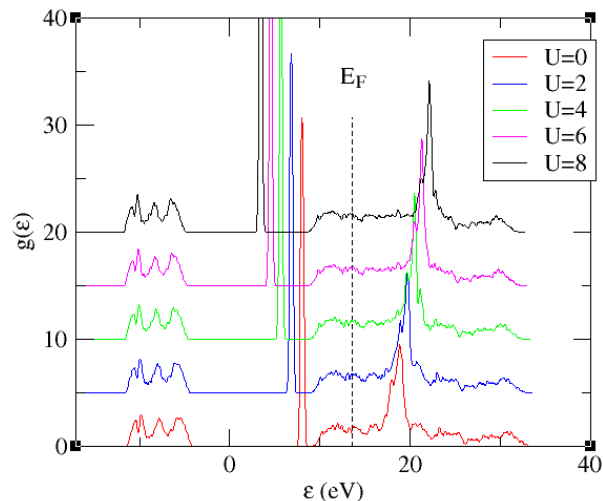


FIG. 5: [supplemental] Calculated Density of States for AFM-Fddd phase with various values of U as shown in eV.

S2. Details of the magnetic free energy calculation

For the magnetic free energy, we calculated the free energy of the Ising model on an fcc lattice with near-

neighbour interaction J .

$$\mathcal{H} = -J \sum_{\langle i,j \rangle'} S_i S_j \quad (1)$$

J can be either positive (ferromagnetic) or negative (antiferromagnetic). We used the effective field approach which gives an analytic, albeit complicated, expression for the free energy.

The parameter J was fitted to the DFT values for the difference in enthalpy between FM and AFM structures. Consequently, J takes a different value for each crystal structure, and is pressure dependent. Where more than one AFM structure was considered, J was fitted to the average value. We note that the enthalpy difference includes the $P\Delta V$ term which arises from the volume difference between FM and AFM. The negative thermal expansion of Gd arises from the fact that as spins flip thermally in the FM-hcp phase, the reduced exchange interaction allows for compression.

Once J is determined, the magnetic contribution to the ground state ($T=0$) energy is fixed. To compare different crystal structures, this is subtracted, so that the enthalpy difference is precisely as given by the DFT.

$$\Delta H_{\alpha,\beta}(T) = \Delta H_{\alpha,\beta}^{DFT}(0) + \Delta H_{\alpha,\beta}^{mag}(T) - \Delta H_{\alpha,\beta}^{mag}(0)$$

S3. Details of the phonon free energy calculation

We carried out phonon free energy calculations in the harmonic approximation using CASTEP. Har-

monic phonon frequencies are calculated using the as-implemented finite displacement lattice dynamics method^{27,41,42} At 0GPa, we compared the stable ferromagnetic hcp phase with the lowest energy (ferrimagnetic) 9R phase. This comprises a double close-packed layer of up-spin followed by a single layer of down-spin, resulting in a macroscopic moment: this arrangement is neither ferromagnetic nor antiferromagnetic, hence the slightly irregular use of the term Ferrimagnetic. It is the lowest enthalpy decoration of spins we found, below ferromagnetic, alternating close-packed layers, and alternating $[11\bar{2}0]$ lines within the close packed layers, the arrangement which maximises the number of opposite-spin pairs

Figure. S6 shows the variation in the phonon contribution to the free energy in the harmonic approximation. The main feature to note is that the hcp and 9R phases are extremely close, e.g. at 300K, 0GPa hcp is -83meV and 9R is -85meV, the 2meV difference is therefore an order of magnitude lower than the magnetic effects. The phonon densities of state themselves are shown in Figure. S7

S4. Examples AFM castep structures

```

AFM-hcp

%block lattice_cart
  3.2170236    1.8573495    -0.0000000
 -0.0000000    3.7146989    -0.0000000
 -0.0000000   -0.0000000    5.9696793
%endblock lattice_cart
%block positions_frac
Gd 0.0000000000 0.0000000000 0.00000000 spin=7.9
Gd 0.3333333333 0.3333333333 0.5 spin=-7.9
%endblock positions_frac

AFM-9R

%block lattice_cart
  8.9699005    -1.8411527    -0.1624865
  8.9699005     1.8411527    -0.1624865
 17.0834975     0.0000000     6.1091634
%endblock lattice_cart
symmetry_generate
snap_to_symmetry
%block positions_frac
Gd 0.0000000 0.0000000 0.0000000 spin=-7.9

```

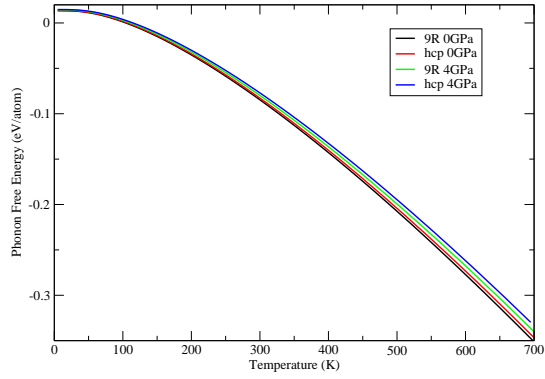


FIG. 6: [supplemental] Quasiharmonic contribution to Phonon Free Energy for 9R and hcp

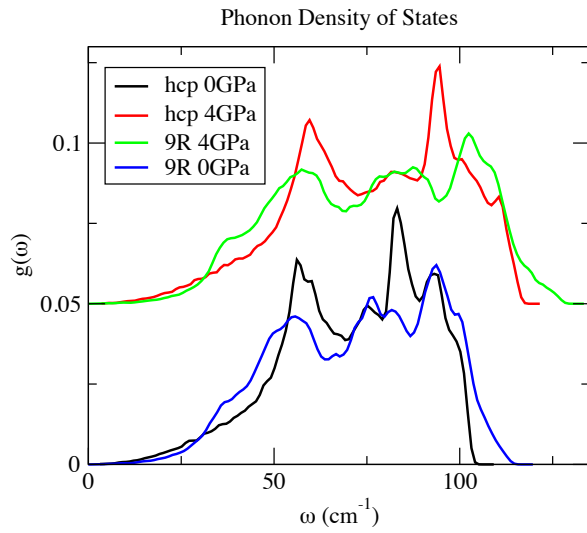


FIG. 7: [supplemental] Phonon densities of states for 9R and hcp at 0GPa and 4GPa (displaced). The zero point energies are 0.01354eV/atom and 0.01450eV/atom for 9R; 0.01365 eV/atom and 0.01470eV/atom for hcp at 0 and 4GPa respectively.

```

Gd    0.222222222  0.222222222  0.111111111  spin=7.9
Gd    0.777777778  0.777777778  0.388888888888  spin=-7.9
Gd    0.0000000    0.0000000    0.5    spin=7.9
Gd    0.222222222  0.222222222  0.611111111111  spin=-7.9
Gd    0.777777778  0.777777778  0.888888888888  spin=7.9
%endblock positions_frac

```

```
%BLOCK lattice_cart
```

```
ANG
```

```

      3.18482849821009      1.83876158342089      0.00000000000000
      3.18482849821009     -1.83876158342089      0.00000000000000
4.24643799693      0.00000000000000      17.906

```

```
%ENDBLOCK lattice_cart
```

```
%block positions_frac
```

```

Gd    0.0000000    0.0000000    0.0000000  spin=7.8
Gd    0.55555555555  0.55555555555  0.16666666666  spin=-7.8
Gd    0.77777777777  0.77777777777  0.33333333333  spin=7.8
Gd    0.0000000    0.0000000    0.5000000  spin=-7.8
Gd    0.55555555555  0.55555555555  0.66666666666  spin=7.8
Gd    0.77777777777  0.77777777777  0.83333333333  spin=-7.8
%endblock positions_frac

```

```
9R-Ferri
```

```
%BLOCK lattice_cart
```

```
ANG
```

```

      2.11879279179908      0.00000000000000      8.86188738887579
     -1.05939639589954      1.83492837184018      8.86188738887579
     -1.05939639589954     -1.83492837184018      8.86188738887579

```

```
%ENDBLOCK lattice_cart
```

```
%BLOCK positions_frac
```

```

Gd    -0.0000000000000000      -0.0000000000000000      -0.0000000000000000  SPIN=-7.800
Gd    0.221418839009061      0.221418839009061      0.221418839009061  SPIN= 7.800
Gd    0.778581160990939      0.778581160990939      0.778581160990939  SPIN= 7.800

```

```
%ENDBLOCK positions_frac
```

```
AFM-fcc
```

```
%BLOCK lattice_cart
```

```
ANG
```

```

      3.60447438475254      0.109501252625182E-35      0.00000000000000
      0.109501252625182E-35      3.60447438475254      -0.144308898241572E-57
      0.0000000000000000     -0.204083601064473E-57      5.24509012894360

```

```
%ENDBLOCK lattice_cart
```

```
%BLOCK positions_frac
```

```

Gd    0.0000000000000000      0.0000000000000000      0.0000000000000000  SPIN= 7.500
Gd    0.5000000000000000      0.5000000000000000      0.5000000000000000  SPIN=-7.500

```

```
%ENDBLOCK positions_frac
```

```
%BLOCK lattice_cart
```

```
ANG
```

```

      2.97633087949342      0.903693904420478E-36     -0.331177716568357E-36
      0.903693904420478E-36      2.97633087949342     -0.332259333440925E-36
     -0.468569060571272E-36     -0.470099393611576E-36      8.6

```

```
%ENDBLOCK lattice_cart
```

```
%BLOCK cell_constraints
  1  1  3
  0  0  0
%ENDBLOCK cell_constraints

%BLOCK positions_frac
Gd      0.0000000000000000    0.0000000000000000    0.0000000000000000 SPIN= 7.500
Gd      0.5000000000000000    0.5000000000000000    0.2500000000000000 SPIN=7.500
Gd      0.0000000000000000    0.0000000000000000    0.5000000000000000 SPIN= -7.500
Gd      0.5000000000000000    0.5000000000000000    0.7500000000000000 SPIN=-7.500
%ENDBLOCK positions_frac

Fddd

%block lattice_cart
  2.8299946    1.5442522    0.0000000
 -0.0000000    3.0885043    0.0000000
  0.0000000    0.0000000    10.3135949
%endblock lattice_cart
symmetry_generate
%block positions_frac
Gd 0.0000000000 0.0000000000 0.0000000000 spin=7.4
Gd 0.5 0.0 0.25 spin=-7.4
Gd 0.0 0.5 0.5 spin=7.4
Gd 0.5 0.5 0.75 spin=-7.4
%endblock positions_frac
```